Journal of Biomechanics 91 (2019) 79–84

Contents lists available at ScienceDirect

Journal of Biomechanics

journal homepage: www.elsevier.com/locate/jbiomech
www.JBiomech.com

A bipedal compliant walking model generates periodic gait cycles with realistic swing dynamics

Hyerim Lim, Sukyung Park [1]

Department of Mechanical Engineering, Korea Advanced Institute of Science and Technology (KAIST), Daejeon, Republic of Korea

ARTICLE INFO

Article history:
Accepted 7 May 2019

Keywords:
Walking
Bipedal
Spring-loaded inverted pendulum
Step length
Swing dynamics
Foot trajectory

ABSTRACT

A simple spring mechanics model can capture the dynamics of the center of mass (CoM) during human walking, which is coordinated by multiple joints. This simple spring model, however, only describes the CoM during the stance phase, and the mechanics involved in the bipedality of the human gait are limited. In this study, a bipedal spring walking model was proposed to demonstrate the dynamics of bipedal walking, including swing dynamics followed by the step-to-step transition. The model consists of two springs with different stiffnesses and rest lengths representing the stance leg and swing leg. One end of each spring has a foot mass, and the other end is attached to the body mass. To induce a forward swing that matches the gait phase, a torsional hip joint spring was introduced at each leg. To reflect the active knee flexion for foot clearance, the rest length of the swing leg was set shorter than that of the stance leg, generating a discrete elastic restoring force. The number of model parameters was reduced by introducing dependencies among stiffness parameters. The proposed model generates periodic gaits with dynamics-driven step-to-step transitions and realistic swing dynamics. While preserving the mimicry of the CoM and ground reaction force (GRF) data at various gait speeds, the proposed model emulated the kinematics of the swing leg. This result implies that the dynamics of human walking generated by the actuations of multiple body segments is describable by a simple spring mechanics.

1. Introduction

A conventional spring-loaded inverted pendulum (SLIP) model can capture the dynamics of the center of mass (CoM) and the ground reaction force (GRF) of human walking. The oscillatory motion of the CoM and GRF can be well described by the response of a simple mass-spring system and the force created by the spring (Geyer et al., 2006; Jung and Park, 2014; Whittington and Thelen, 2009). Moreover, increasing the oscillatory response of the CoM and corresponding GRF with gait speed in both young and elderly subjects and loading conditions has been demonstrated by increasing leg stiffness with gait speed (Hong et al., 2013; Kim and Park, 2011; Lee et al., 2014). The stability of upright human walking was examined using a SLIP model with the expansion of the CoM point to a rigid body with a virtual pivot point that creates external support (Maus et al., 2010). Recently, the motion of multiple lower limbs of stance leg that generates oscillation the CoM was described by a SLIP model with compliantly connected-curvy foot (Lim and Park, 2018). In this manner, spring mechanics could serve as a mechanical template for understanding the dynamics of human walking.

The SLIP model in contact with the ground, however, demonstrates the mechanics of the CoM during the stance phase only. To demonstrate the step-to-step transition of bipedal human walking, the placement of the ground contact of the leading leg during double-support phase must be predetermined as a form of angle of attack (Geyer et al., 2006; Kim and Park, 2011; Whittington and Thelen, 2009). Therefore, the SLIP model is limited in describing the mechanics related to bipedality, such as the dynamic generation of step-to-step transition, mechanics involved in step length-speed relationships, etc. To incorporate bipedalism into the SLIP model, recent studies have introduced a rigid swing pendulum walking on a slope or connected to the stance leg with a torsional spring (Charles et al., 2017; Gan et al., 2018). Although these models have successfully generated various bipedal gaits, such as walking, running and skipping, the rigid swing leg moves through the ground to make a step-to-step transition, which is very different from that of human locomotion. Moreover, the rigid pendulum does not emulate the force profiles of human gait, unlike the spring pendulum. Therefore, to understand the force and motion relationship of the bipedal human walking, it would be beneficial to establish a simple mechanical model, if possible, that

[1] Department of Mechanical Engineering, KAIST, 291 Daehak-ro, Yuseong-gu, Daejeon 34141, Republic of Korea.

E-mail address: sukyungp@kaist.ac.kr (S. Park)

https://doi.org/10.1016/j.jbiomech.2019.05.020
0021-9290/

demonstrates the resultant force and motion relationship, i.e., the dynamics of human walking, which is in fact actuated and coordinated by multiple joints in a complex manner.

In this study, we proposed a bipedal spring walking model that emulates the kinetics and kinematics of the step-to-step transition of human walking and numerically found limit cycles near the preferred gait speed ranges. The model consists of a point CoM supported by two springy legs of stance leg and swing leg connected by a torsional hip spring to the CoM. To demonstrate the dynamics of the swing leg while not significantly altering the CoM dynamics, a very small foot mass was placed at the end of each leg spring. To demonstrate the onset of swing leg flexion at the beginning of the swing phase, a discrete elastic restoring force was introduced. The simulation results of kinematics and kinetics of the model were compared with human walking data.

2. Methods

2.1. Bipedal spring walking model

We proposed a double springy legged walking model to demonstrate bipedal walking with automatic step-to-step transition (Fig. 1A, B). To generate foot clearance while matching the swing phase, a minimal complexity was added to the conventional SLIP model as a form of swing leg spring and an interleg torsional spring (Fig. 1C, D). Specifically, the model consists of two springs of varying stiffness k and rest length l_0 representing the stance leg and swing leg (Fig. 1A). The subscripts 1 and 2 indicate the stance and swing leg, respectively, throughout the manuscript. At the onset of the double-support phase, the previous swing leg becomes another leading stance leg and is denoted an additional subscript 'lead'. One end of each spring has a foot mass of m, and the other end is attached to the body mass, M. To induce a forward swing that matches the gait phase while being cued by the observed proportionality between the hip joint torque and angle (Shamaei et al., 2013), a torsional hip joint spring of stiffness k_r was introduced into each leg (Fig. 1C)). To reflect the active knee flexion for foot clearance, the rest length of the swing leg was set to be different from that of the stance leg to generate forces to lead leg shortening (Fig. 1D).

The equations of motion of the proposed model were obtained from Newton's equation and kinematic constraints as follows:

$$\mathbf{M}\ddot{\mathbf{q}} = \mathbf{V} + \boldsymbol{\tau} \tag{1}$$

where the state vector $\mathbf{q}$, the mass matrix $\mathbf{M}$, and velocity matrix $\mathbf{V}$ for the single-stance phase (Eq. (1a)) and the double-support phase (Eq. (1b)) are listed below.

$$\mathbf{q} = [l_1 \quad \theta_1 \quad l_2 \quad \theta_2]^T$$

$$\mathbf{M} = \begin{bmatrix} M\sin\theta_1 & Ml_1\cos\theta_1 & 0 & 0 \\ M\cos\theta_1 & -Ml_1\sin\theta_1 & 0 & 0 \\ m\sin\theta_1 & ml_1\cos\theta_1 & -m\sin\theta_2 & -ml_2\cos\theta_2 \\ m\cos\theta_1 & -ml_1\sin\theta_1 & -m\cos\theta_2 & ml_2\sin\theta_2 \end{bmatrix}$$

$$\mathbf{V} = \begin{bmatrix} M(l_1\dot{\theta}_1^2\sin\theta_1 - 2\dot{l}_1\dot{\theta}_1\cos\theta_1) \\ M(l_1\dot{\theta}_1^2\cos\theta_1 + 2\dot{l}_1\dot{\theta}_1\sin\theta_1) \\ m(l_1\dot{\theta}_1^2\sin\theta_1 - 2\dot{l}_1\dot{\theta}_1\cos\theta_1 - l_2\dot{\theta}_2^2\sin\theta_2 + 2\dot{l}_2\dot{\theta}_2\cos\theta_2) \\ m(l_1\dot{\theta}_1^2\cos\theta_1 + 2\dot{l}_1\dot{\theta}_1\sin\theta_1 - l_2\dot{\theta}_2^2\cos\theta_2 - 2\dot{l}_2\dot{\theta}_2\sin\theta_2) \end{bmatrix}$$

$$\boldsymbol{\tau} = \begin{bmatrix} k_1(l_{01} - l_1)\sin\theta_1 + k_2(l_{02} - l_2)\sin\theta_2 - (k_r\theta_1/l_1)\cos\theta_1 - (k_r\theta_2/l_2)\cos\theta_2 \\ k_1(l_{01} - l_1)\cos\theta_1 + k_2(l_{02} - l_2)\cos\theta_2 + (k_r\theta_1/l_1)\sin\theta_1 + (k_r\theta_2/l_2)\sin\theta_2 - Mg \\ -k_2(l_{02} - l_2)\sin\theta_2 + (k_r\theta_2/l_2)\cos\theta_2 \\ -k_2(l_{02} - l_2)\cos\theta_2 - (k_r\theta_2/l_2)\sin\theta_2 - mg \end{bmatrix} \tag{1a}$$

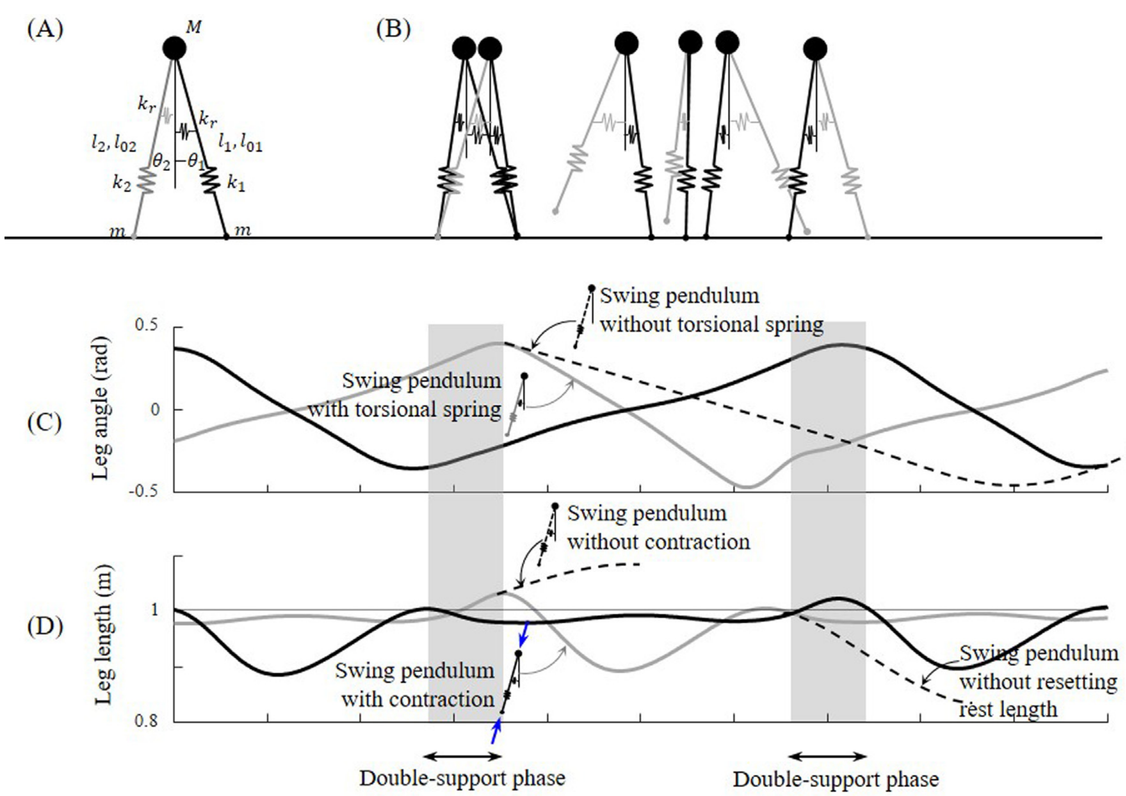

Fig. 1. Schematics of the proposed bipedal compliant walking model. (A) The model consists of two springs that represent the stance leg (black) and swing leg (gray) connected by a torsional hip joint spring of stiffness k_r, with a foot mass and body mass attached to the end of each spring. (B) The model configuration at different gait phases from double- to single-support phases. Alternate legs are represented by black and gray lines. (C) Time trajectories of the leg angle and (D) the leg length of averaged experimental data of ten subjects. The dashed lines in (C) and (D) are the trajectory of the swing leg angle without torsional spring and discrete shortening of the rest length of the swing spring, respectively.

where the state variables l and θ are the springy leg length and the leg angle from the vertical, with a positive sign representing the counterclockwise direction.

$$\begin{aligned}
&\mathbf{q} = [l_1 \quad \theta_1]^T \\
&\mathbf{M} = \begin{bmatrix} M\sin\theta_1 & Ml_1\cos\theta_1 \\ M\cos\theta_1 & -Ml_1\sin\theta_1 \end{bmatrix} \\
&\mathbf{V} = \begin{bmatrix} M(l_1\dot{\theta}_1^2\sin\theta_1 - 2\dot{l}_1\dot{\theta}_1\cos\theta_1) \\ M(l_1\dot{\theta}_1^2\cos\theta_1 + 2\dot{l}_1\dot{\theta}_1\sin\theta_1) \end{bmatrix} \\
&\boldsymbol{\tau} = \begin{bmatrix} k_1(l_{01}-l_1)\sin\theta_1 + k_{1,lead}(l_{01,lead}-l_{1,lead})\sin\theta_{1,lead} \\ \quad -(k_r\theta_1/l_1)\cos\theta_1 - (k_r\theta_{1,lead}/l_{1,lead})\cos\theta_{1,lead} \\ k_1(l_{01}-l_1)\cos\theta_1 + k_{1,lead}(l_{01,lead}-l_{1,lead})\cos\theta_{1,lead} \\ \quad +(k_r\theta_1/l_1)\sin\theta_1 + (k_r\theta_{1,lead}/l_{1,lead})\sin\theta_{1,lead} - Mg \end{bmatrix}
\end{aligned} \tag{1b}$$

The nonholonomic constraint (Eq. (1c)) during the double-support phase is obtained as follows:

$$\begin{aligned}
&\mathbf{M}_1\ddot{\mathbf{q}}_1 + \mathbf{V}_1 = \mathbf{M}_{1,lead}\ddot{\mathbf{q}}_{1,lead} + \mathbf{V}_{1,lead} \\
&\mathbf{q}_i = [l_i \quad \theta_i]^T, \quad \mathbf{M}_i = \begin{bmatrix} \sin\theta_i & l_i\cos\theta_i \\ \cos\theta_i & -l_i\sin\theta_i \end{bmatrix}, \\
&\mathbf{V}_i = \begin{bmatrix} 2\dot{l}_i\dot{\theta}_i\cos\theta_i - l_i\dot{\theta}_i^2\sin\theta_i \\ -2\dot{l}_i\dot{\theta}_i\sin\theta_i - l_i\dot{\theta}_i^2\cos\theta_i \end{bmatrix}
\end{aligned} \tag{1c}$$

2.2. Model simulation and parameters

The model simulation was performed from the double- to single-support phase as the following process (Fig. 1(B)). When the swing foot hits the ground in front of the CoM, satisfying the following constraint,

$$l_1\cos\theta_1 = l_2\cos\theta_2, \quad \theta_2 > 0 \tag{2a}$$

the double-support phase is initiated and the swing leg spring variables l_2 and θ_2 change to the leading stance leg spring variables $l_{1,lead}$ and $\theta_{1,lead}$, i.e., $l_2 = l_{1,lead}$, $\theta_2 = \theta_{1,lead}$. The time rate of change in leg length and leg angle of the leading stance leg, $\dot{l}_{1,lead}$, $\dot{\theta}_{1,lead}$, are determined by the nonholonomic constraint of the body mass, M, defined from the two stance legs (Eq. (1c)). The dynamics of the CoM during the double-support phase are integrated until the vertical GRF, F_y, applied to the trailing stance foot becomes to zero as follows,

$$F_y = mg + k_1(l_{01} - l_1)\cos\theta_1 + (k_r\theta_1/l_1)\sin\theta_1 = 0 \tag{2b}$$

Then, the single-support phase is initiated by switching the trailing stance leg to the swing leg spring. The single-support phase is continued until the condition of swing foot ground contact (Eq. (2a)) is satisfied. The limit cycle of the model was numerically determined until the norm of the difference between the fixed-point candidates became less than 0.001.

The system features seven model parameters: M, m, k_1, k_2, k_r, l_{01}, and l_{02}. The mass m and M and the rest length of the stance leg, l_{01}, were set to values similar to those of human body parameters, i.e., 0.015BM and 0.97BM (Clauser et al., 1969), where BM = 80 kg and 1 m, respectively. Previous studies have reported that the leg stiffness k_1 is proportional to gait speed (Kim and Park, 2011) and that the ratio $k_1/M = \omega_1^2 = \omega_n^2$, where ω_n is the natural frequency of the spring pendulum, tends to be maintained regardless of body weight (Lee et al., 2014). With the natural frequencies of the swing leg and torsional spring defined as $k_2/m = \omega_2^2$ and $k_r/m = \omega_r^2$, respectively, the reciprocity between the swing and stance phases could be approximated as $\omega_2 \sim \omega_n$, and interleg swing occurring approximately once per step could be approximated by the swing frequency relationship $\omega_r \sim \omega_n/2$. Using these approximations to simplify the model, three free model parameters of spring stiffness k_1, k_2, and k_r were constrained to have a constant ratio, i.e., $k_1/M = k_2/m = 4k_r/m$, enabling model simulations to be performed with only the free stiffness parameter, k_1. To reflect the active knee flexion for foot clearance, the rest length of the swing leg was set to be shorter than that of the stance leg, i.e., $l_{02} = \alpha \cdot l_{01}$, where $0 < \alpha < 1$. At the beginning and end of the swing phase, the stiffness and rest length of the stance leg switches from k_1 and l_{01} to those of the swing leg, i.e., k_2, l_{02}, and vice versa. The discrete change in the rest length of the spring introduces a discrete elastic contraction force to the swing foot mass m while maintaining continuous state variables l and θ. Finally, the two reduced free model parameters k_1 and α were tuned to mimic human data using grid simulation. Selected model parameters at different gait speeds are listed in Table 1.

Table 1
Normalized values of model parameters for gait simulation at various speeds.

Global: BM = 80 kg, l_{01} = 1 m		
v	ω_n (rad/s)	α
0.32	18.03	0.93
0.35	19.04	0.92
0.38	20.31	0.92

2.3. Experiment

To validate the proposed model, simulation data were compared to empirical motions of the CoM as well as feet, GRF and hip joint force data collected from walking trials in previous studies (Jung and Park, 2014; Lee et al., 2014). Ten young and healthy male subjects (body mass of 73.4 ± 7.83 kg and leg length of 0.90 ± 0.04 m) with no history of gait disorders participated in the walking experiments. The subjects signed informed consent forms before data collection, and the study was approved by the KAIST IRB. During the trials, the subjects walked on a walkway at their natural (1.3 m/s), maximum (1.9 m/s) and moderate (1.6 m/s) speeds in random order. For a steady gait, a gait frequency that corresponds to the subjects' preferred gait speed was guided by a metronome. The ground reaction forces under each foot were measured with a force plate (AMTI, Accugait®) at a sampling rate of 200 Hz. These data were filtered with a Butterworth fifth-order low-pass filter with a cut-off frequency of 10 Hz to eliminate high-frequency noise without significant filtering distortion of the data. Joint kinematics were measured by a motion capture system (Motion Analysis Hawk®) at a sampling rate of 200 Hz and were filtered with a Butterworth fifth-order low-pass filter with a cut-off frequency of 10 Hz. Joint force was calculated by the inverse dynamics of the seven-segment model, which includes the hip, knee, and ankle. The details of the test protocols and data measurements have been reported previously (Jung and Park, 2014; Lee et al., 2014).

3. Results

The bipedal compliant walking model automatically generated periodic gait cycles under its own dynamics. Repeated walking through consecutive touchdowns of the swing leg was numerically determined at speeds ranging from 1.0 m/s to 1.2 m/s, or from 0.32 to 0.38 if normalized by $\sqrt{gl_{01}}$, (Fig. 2). The model simulation of oscillatory CoM trajectories, the forward over-the-ground foot excursion, and the corresponding hip joint forces of each leg qualitatively mimic the human data (Fig. 2). The peak values of the CoM and joint forces increased with gait speed. Quantitatively, however, the magnitude of the spring force of the swing leg was much smaller than that indicated by the data (Fig. 2D) due to the model simplification of the massless swing leg spring with a small foot mass

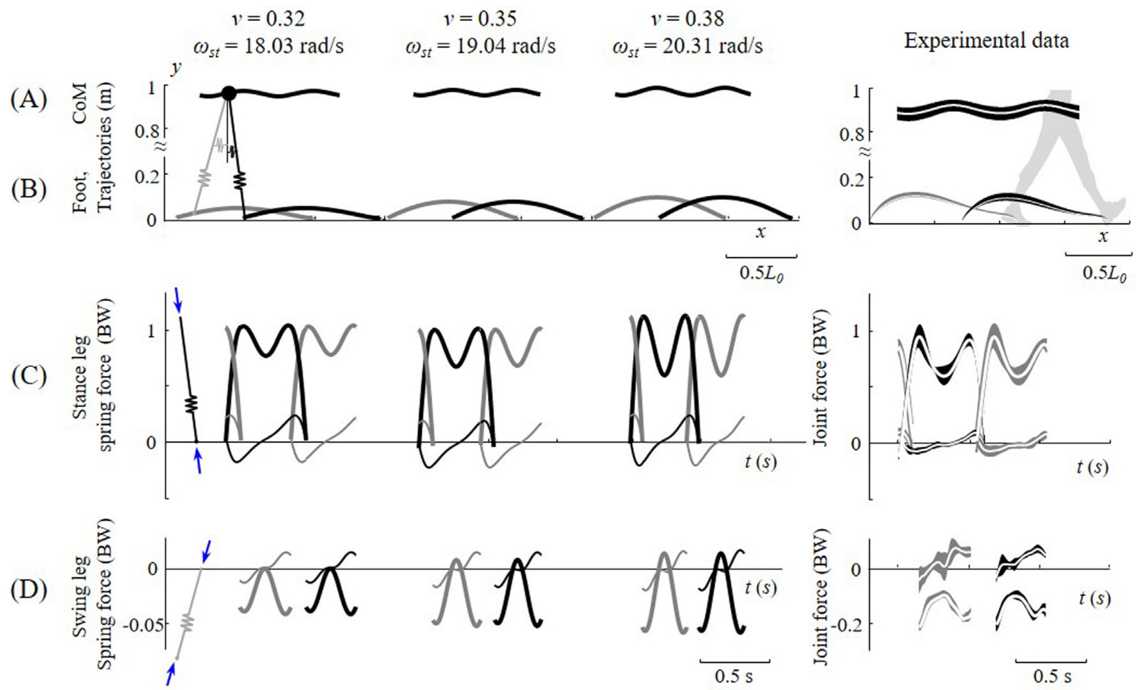

Fig. 2. Kinematic and kinetic data of the CoM during bipedal walking from model simulation (left three columns) and experiment (right). (A) CoM trajectories, (B) foot trajectories, (C) stance leg spring forces (model) and joint forces (experiment), and (D) swing leg spring force (model) and joint forces (experiment). Alternate legs are represented by black and gray lines. The vertical and horizontal directional components of forces are represented by thick and thin solid lines, respectively. The model parameters used for the simulation are listed in Table 1. The experimental data were collected at the ten subjects' preferred speed of approximately 1.3 m/s.

attached to the end. The time trajectories of the state variables, such as leg length, leg angle, and their time rates, in the model simulation and experimental data shared qualitative and quantitative similarities (Fig. 3), whereas the asymmetry of the leg configuration of the data was not emulated by the model. The solution grids of the numerically obtained limit cycles are presented as a function of gait velocity (Fig. 4). The stiffness tends to increase with gait speed, as does the step length, under the constant-stiffness conditions.

4. Discussion

In this study, we examined whether the dynamics of bipedal walking generated by sequential step-to-step transition could be described by simple spring mechanics. We expanded the conventional SLIP model with another compliant swing leg and interleg torsional springs. To reflect active knee flexion at the onset of the swing phase in a simple manner, we introduced a discrete change in rest length between the stance and the swing leg springs, which resulted in an application of a discrete contraction force to the swing leg (Fig. 1). In this manner, the state variables of leg length and angle changed continuously during the transition between the stance and swing phase (Fig. 3). The proposed model could generate sequential bipedal walking under its own dynamics, and the limit cycles were numerically determined over preferred gait speed ranges (Fig. 2). The model simulation showed oscillatory CoM behavior, human-like foot trajectories, corresponding GRFs, and hip joint forces qualitatively similar to those indicated by human data (Fig. 2). In those data (Hong et al., 2013; Jung and Park, 2014; Kim and Park, 2011; Lee et al., 2014), the magnitudes of the CoM oscillation, step length, and the peak GRFs scale with the gait speed (Fig. 2).

One of the benefits of this model is a simple mechanical representation of the force and motion relationship, i.e., the dynamics of bipedal human walking, which is in fact controlled by multiple joints in a complex manner. Compared to the previous mechanical representation of human walking, the proposed model generates automatic step-to-step transitions and realistic foot trajectories. Previous SLIP models require that the step-to-step transition be arbitrarily set in a predetermined manner (Geyer et al., 2006; Jung and Park, 2014; Whittington and Thelen, 2009) and are limited in examining the dynamics of bipedalism, such as the dynamics related to the step-to-step transition or the relationship between the gait speed and step length. Recently, a bipedal walking model in the form of a rigid swing leg attached to a springy stance leg with a torsional spring was introduced to generate an automatic step-to-step transition (Gan et al., 2018). In the mid-stance, the rigid pendulum generates under-the-ground foot trajectories, which is very different from human walking. On the other hand, the proposed model demonstrated the halfway realistic foot clearance of the swing dynamics (Fig. 3). The proposed model could predict the speed proportional increase in step length similar to that observed in human data (Kuo, 2001), although the model was examined over a very limited range of walking speeds (Fig. 4). Recalling that the newly introduced springy swing leg generated profiles of interleg angle, leg length changes, and hip joint forces similar to those observed in empirical data (Figs. 2 and 3), these results indicate that the both swing and stance leg dynamics during human walking are well mimicked by a simple point mass and spring mechanics.

Although the proposed model could demonstrate a bipedal gait and related force and motion relationship, steady solutions were obtained within a very narrow range of walking speeds (Fig. 4), which appears to be attributed to the simplified model parameters. To simplify the model, the three free model parameters of spring stiffness k_1, k_2, and k_r were constrained to have a constant ratio, i.e., $k_1/M = k_2/m = 4k_r/m$, such that the model simulation was performed with only the free stiffness parameter, k_1. Considering that

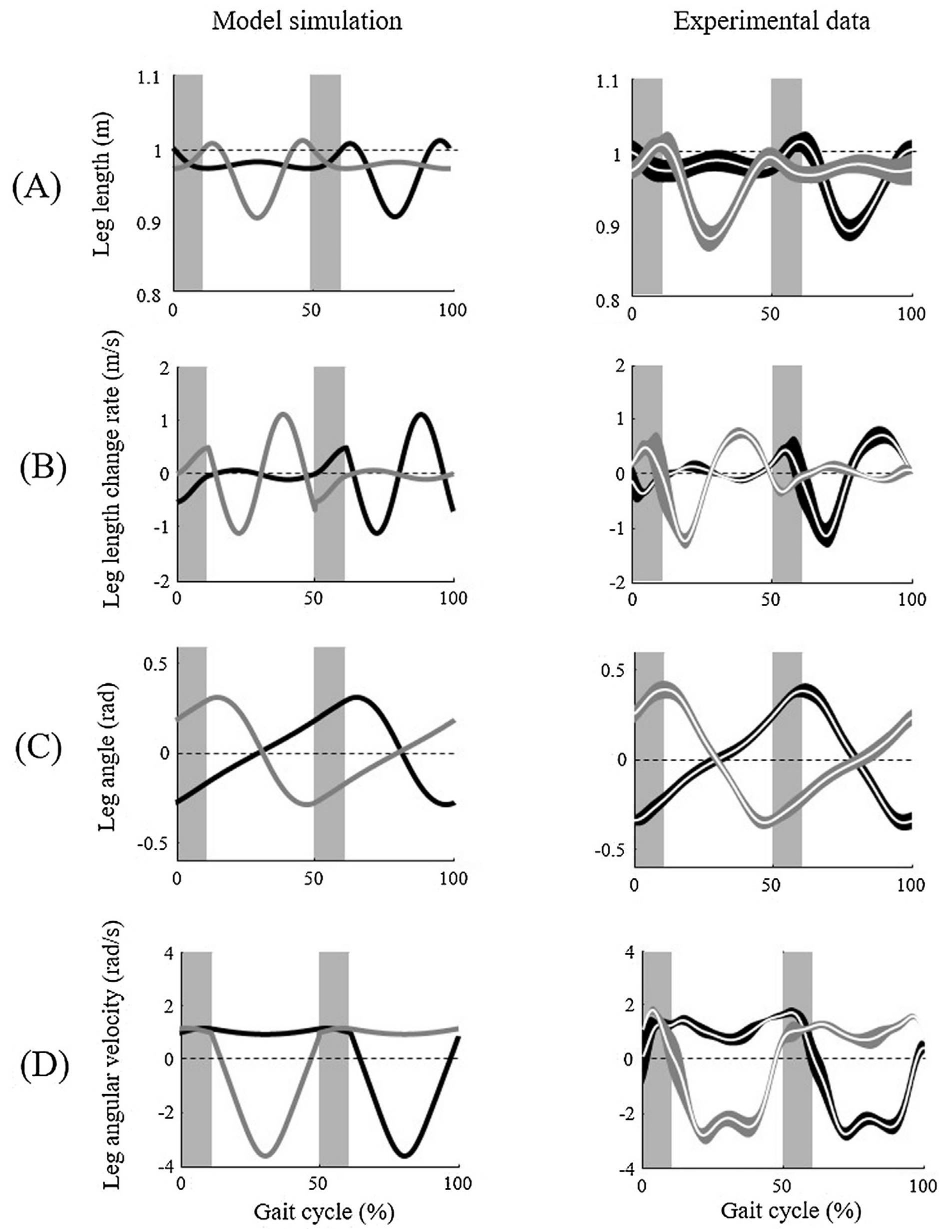

Fig. 3. Kinematic data of the stance and swing leg from model simulation (left) and experiment (right). The trajectories of (A) leg length, (B) time rate of leg length change, (C) leg angle, and (D) angular velocity of leg. Alternate legs are represented in black and gray, respectively, and white lines indicate the average of ten subjects' data, with the standard deviations shown as shaded bars.

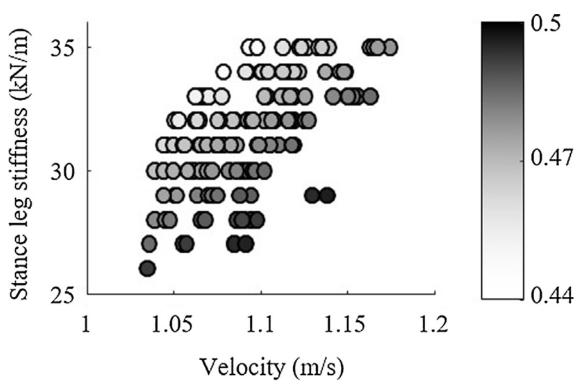

Fig. 4. The solution grids of the limit cycles as a function of walking speed. The grayscale color of the filled circle indicates the magnitude of the step length.

the previous SLIP model operates with two free parameters of stiffness k and predetermined step length in terms of touchdown angle α, the current model expands the describability of human walking without significantly increasing model complexity. By having the stiffness ratio be an additional free model parameter, for example, increasing the torsional spring stiffness, k_r, by 10%, steady walking solutions were obtained up to a speed of 1.4 m/s (not shown), similar to the steady solutions obtained for a rigid-pendulum walking model (Kuo, 2002). Therefore, one may obtain the steady walking solutions of the model over a broader range with more model parameters at the expense of model complexity. Whereas the motion of the swing leg well emulated the human data, the joint forces of the swing leg showed a great quantitative discrepancy from the data by an order of magnitude (Fig. 2) because of the unrealistically small swing leg inertia. To maintain the reproducibility of the CoM dynamics using the conventional SLIP model (Geyer et al., 2006; Jung and Park, 2014; Kim and Park, 2011; Lee et al., 2014; Lim and Park, 2018; Whittington and Thelen, 2009), the coupling effect between the added swing leg inertia and the CoM dynamics was minimized by setting the swing leg to a massless leg with a small foot mass. It is worth noting that the good reproducibility of the data by the proposed model does not indicate that the spring mechanics or any introduced mechanics underlie human walking. For example, the employment of a discrete spring force to generate swing leg flexion is not physiologically supportive. Neither knee joint torque nor knee flexor EMG showed any significant increase during the swing phase of gait (Neptune et al., 2001). The knee joint angle continued to increase flexion due to the forward movement of the swing inertia following the weight shift to the stance leg, not by the active flexion torque. One final thing to note is that the proposed model is not a conservative system. To achieve active knee flection and extension at the beginning and end of the swing phase in a simple manner, we introduced a discrete inflow and outflow of elastic potential energy by resetting the resting spring length. The amount of elastic energy flow during the swapping of the rest length of the spring was relatively small compared to the total mechanical energy of the entire system (0.1–0.3% of total mechanical energy during the double-support phase). The collision loss of the swing foot mass during ground contact was also negligible because the swing foot velocity nearly reached zero at collision.

In conclusion, we proposed a spring-based mechanical model that generates the repeated gait cycles of bipedal walking under its own dynamics with realistic swing dynamics. The simple spring mechanics emulated the force and motion relationship and the speed and step length relationship of bipedal walking. The results imply that a simple spring mechanics could serve as a mechanical template for understanding the force and motion relationship of bipedal human walking, which is in fact actuated by multiple muscles and coordinated by multiple joints.

Declaration of Competing Interest

None.

Acknowledgements

This work was supported by the BK21 PLUS program, the G-CORE project (N11190032), and a National Research Foundation of Korea (NRF) grant funded by the Korean government (MSIT) (No. 2016R1A2B4007224). We thank C. David Remy and anonymous reviewers for their insightful comments, which greatly helped us improve the manuscript.

References

Charles, W., Ransing, R., Sazonov, I., Friswell, M., 2017. A passive spring-mass model with rolling contact and leg masses to investigate the ballistics of swing dynamics.

Clauser, C.E., McConville, J.T., Young, J.W., 1969. Weight, volume, and center of mass of segments of the human body. Antioch Coll Yellow Springs OH.

Gan, Z., Yesilevskiy, Y., Zaytsev, P., Remy, C.D., 2018. All common bipedal gaits emerge from a single passive model. J. R. Soc. Interface 15.

Geyer, H., Seyfarth, A., Blickhan, R., 2006. Compliant leg behaviour explains basic dynamics of walking and running. Proc. Biol. Sci. 273, 2861–2867.

Hong, H., Kim, S., Kim, C., Lee, S., Park, S., 2013. Spring-like gait mechanics observed during walking in both young and older adults. J. Biomech. 46, 77–82.

Jung, C.K., Park, S., 2014. Compliant bipedal model with the center of pressure excursion associated with oscillatory behavior of the center of mass reproduces the human gait dynamics. J. Biomech. 47, 223–229.

Kim, S., Park, S., 2011. Leg stiffness increases with speed to modulate gait frequency and propulsion energy. J. Biomech. 44, 1253–1258.

Kuo, A.D., 2002. Energetics of actively powered locomotion using the simplest walking model. J. Biomech. Eng. 124, 113.

Kuo, A.D., 2001. A simple model of bipedal walking predicts the preferred speed-step length relationship. J. Biomech. Eng. 123, 264.

Lee, M., Kim, S., Park, S., 2014. Resonance-based oscillations could describe human gait mechanics under various loading conditions. J. Biomech. 47, 319–322.

Lim, H., Park, S., 2018. Kinematics of lower limbs during walking are emulated by springy walking model with a compliantly connected, off-centered curvy foot. J. Biomech. 71, 119–126.

Maus, H.M., Lipfert, S.W., Gross, M., Rummel, J., Seyfarth, A., 2010. Upright human gait did not provide a major mechanical challenge for our ancestors. Nat. Commun. 1, 70.

Neptune, R., Kautz, S., Zajac, F., 2001. Contributions of the individual ankle plantar flexors to support, forward progression and swing initiation during walking. J. Biomech. 34, 1387–1398.

Shamaei, K., Sawicki, G.S., Dollar, A.M., 2013. Estimation of quasi-stiffness of the human hip in the stance phase of walking. PloS One 8, e81841.

Whittington, B.R., Thelen, D.G., 2009. A simple mass-spring model with roller feet can induce the ground reactions observed in human walking. J. Biomech. Eng. 131, 011013.